retained at their original value. This eliminated >95% of the low-TFI background pixels. The threshold value was <10% of that predicted for one probe molecule (five CY3 fluorochromes) and when applied to the experimental image did not adversely affect the value from one hybridized probe. Brighter background pixels that eluded the thresholding filter but whose TFI value was less than that for one hybridized probe were excluded during the mapping analysis. The result was a filtered image where one hybridized CY3 labeled probe could be distinguished.

20. Data Analysis and Visualization Environment (DAVE); copyright 1995 by Lawrence M. Lifshitz and the University of Massachusetts Medical School.
21. The reassignment of light to a point source in a restoration results in one or two brighter voxels at the location of the point source in addition to a number of associated contiguous voxels. A point source is thus described as an object comprising a group of contiguous nonzero voxels in a restored image after thresholding. All the nuclear and cytoplasmic point sources therefore had a finite size and were treated as three-dimensional objects.
22. Additional evidence that every discrete signal is a single RNA molecule is that, when each of the five probes was hybridized individually, analysis showed that >95% of the detected sites had one probe hybridized. When two probes to the 3′-UTR were used, a population of single and double probes was detected (*6*). As an additional control, a set of five probes to an mRNA not expressed in these cells (α-actin) gave about 20 single probe signals per cell (2% of the β-actin single probe signal), but no multiple probe signals when processed by identical methods.
23. Supplementary material is available at www.sciencemag.org/feature/data/975399.shl. General information is available at www.singerlab.aecom.yu.edu.
24. We thank members of the Biomedical Imaging Facility, L. M. Lifshitz and J. Collins for their assistance with the DAVE software, R. A. Tuft for carrying out the light-flux measurements of the microscope, Y.-L. Wang for NRK cells, and K. Taneja for oligonucleotide probe synthesis. Supported by NIH grant GM 54887 to R.H.S. We are deeply saddened by the loss of our colleague and close friend Fredric S. Fay during the preparation of this manuscript.

3 October 1997; accepted 20 February 1998

In Situ Visualization of DNA Double-Strand Break Repair in Human Fibroblasts

Benjamin E. Nelms,* Richard S. Maser,* James F. MacKay, Max G. Lagally, John H. J. Petrini†

A method was developed to examine DNA repair within the intact cell. Ultrasoft x-rays were used to induce DNA double-strand breaks (DSBs) in defined subnuclear volumes of human fibroblasts and DNA repair was visualized at those sites. The DSBs remained in a fixed position during the initial stages of DNA repair, and the DSB repair protein hMre11 migrated to the sites of damage within 30 minutes. In contrast, hRad51, a human RecA homolog, did not localize at sites of DNA damage, a finding consistent with the distinct roles of these proteins in DNA repair.

Proteins that mediate certain aspects of DNA metabolism, such as DNA replication, appear to be compartmentalized within the nucleus. DNA replication therefore requires the movement of DNA to and from established sites within the nuclear matrix (*1*). Cytologic analyses have revealed that the DSB repair proteins hRad51 and the hMre11-hRad50 complex assemble in discrete nuclear foci as part of the normal cellular response to DNA damage (*2–5*). These findings may indicate that DNA repair does not entail the movement of DNA DSBs to preexisting intranuclear sites. Rather, they suggest that DNA repair proteins move to sites of DNA damage. The inability to detect DSBs in situ has made it difficult to address this issue experimentally. A method to induce and subsequently detect DSBs within a defined subnuclear volume would, in principle, provide a means to determine whether DSB repair requires the movement of DNA repair proteins to the sites of DNA damage.

To that end, we developed a method to examine the temporal and spatial nature of DSB repair within the context of the intact cell. This method relies on synchrotron-generated ultrasoft x-rays [<5000 electron volts (5 keV)], a multilayer monochromator for tunable ultrasoft x-ray energies with sufficient intensity for irradiation of live human fibroblasts (*6*), and microfabricated irradiation masks to induce DNA damage in discrete subnuclear regions of irradiated cells (Fig. 1) (*7*). The irradiation masks were fabricated with x-ray lithography and consist of gold stripes (1.85 μm wide with 1.35-μm separation) deposited on thin Si_2N_4 membranes (*7*). Dosimetric analyses with the irradiation mask showed that gold-shielded regions receive about 0.5% of the dose absorbed by the nonshielded regions (*7*). Irradiated cells thus absorb ultrasoft x-rays in 1.35-μm-wide stripes separated by 1.85-μm gaps that remain essentially unirradiated.

The 1.34-keV ultrasoft x-rays used in these experiments act almost exclusively through photoelectric interactions in biological material (*8*), resulting in low-energy electrons that have very short track lengths (<50 nm), comparable to the dimensions of biologically relevant structures such as chromatin (*9*). These properties suggested that photoelectrons and Auger electrons as well as free radicals resulting from absorption of ultrasoft x-rays would induce DNA damage almost exclusively within the 1.35-μm stripes imposed by the grids. Human fibroblasts (37Lu) were irradiated and DSBs were labeled with bromodeoxyuridine triphosphate (BrdU) and terminal deoxynucleotidyltransferase (TdT) for visualization with fluorescein isothiocyanate (FITC)–conjugated monoclonal antibody to BrdU (FITC–anti-BrdU) 30, 90, or 300 min later (*10–12*). Under the conditions used, TdT does not label single-strand DNA nicks (*12*). Nuclei observed 30 min after irradiation displayed a strong FITC signal in parallel stripes corresponding to BrdU incorporation at DNA ends (Fig. 2A). Each pair of unirradiated-irradiated stripes is 3.2 μm wide (1.85 μm unirradiated plus 1.35 μm irradiated). Hence, most nuclei (average diameter 15 to 20 μm) contained six or seven FITC-staining stripes (Fig. 2, A and B). Confocal microscopy demonstrated that parallel stripes of BrdU incorporation were uniform through-

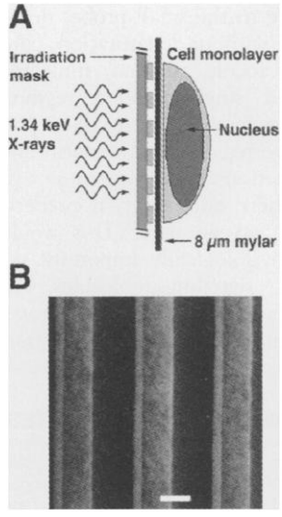

Fig. 1. (**A**) Diagram of the partial volume irradiation scheme (*7*). Thickness of the Mylar surface (8 μm) is not drawn to scale. (**B**) Scanning electron micrograph of irradiation mask. Bar, 1 μm.

B. E. Nelms, Laboratory of Genetics and Department of Medical Physics, University of Wisconsin Medical School, Madison, WI 53706, USA.
R. S. Maser and J. H. J. Petrini, Laboratory of Genetics, University of Wisconsin Medical School, Madison, WI 53706, USA.
J. F. MacKay and M. G. Lagally, Department of Materials Science and Engineering, University of Wisconsin, Madison, WI 53706, USA.

*These authors contributed equally to this work. Names are listed in random order.
†To whom correspondence should be addressed. E-mail: jpetrini@facstaff.wisc.edu

out the volume of the nucleus at this time point (Fig. 2, F to I) (*13*). These data indicate that ultrasoft x-rays induce highly localized DNA damage in living cells.

The FITC signal corresponding to BrdU-labeled DSBs disappeared between 90 (Fig. 2, C and D) and 300 min (*14*) after irradiation. Single cell electrophoresis (comet) assays revealed that the failure to detect FITC stripes at later time points was due to repair rather than redistribution of the DSBs (*15*). Similar DSB repair kinetics were previously observed after ultrasoft x-irradiation without an irradiation mask (*16*).

We reasoned that if DSBs were largely stationary before repair, their persistence in a DNA repair-deficient cell would lead to the persistence of DSB stripes. To test this hypothesis, we stripe-irradiated the DSB repair-deficient human fibroblast cell line 180BR (*17*), BrdU-labeled DNA DSBs with TdT, and stained the cells with FITC–anti-BrdU to visualize DSBs. In contrast to 37Lu cells, in which BrdU incorporation was undetectable by 90 min postirradiation, the 180BR cells had readily observable FITC–anti-BrdU stripes as late as 300 min postirradiation (Fig. 2E). Previous analyses had shown that minimal DSB repair occurs over this time course in 180BR cells (*2*, *17*). These data indicate that DSBs are held in a relatively fixed position, at least in the early stages of DNA repair, and suggest that the bulk of DSB repair does not involve movement of DNA lesions through intranuclear space. In this regard, DSB repair differs from DNA replication, which is mediated by compartmentalized nuclear proteins (*1*). Instead, the spatial behavior of DSBs suggested that DSB repair requires the recruitment of DSB repair proteins to sites of damaged DNA.

To test this hypothesis, we examined whether two DSB repair complexes, one that includes hMre11 and hRad50 and another that includes hRad51, were recruited to the site of DSBs. Several criteria indicate that these protein complexes, both of which form nuclear foci in response to the induction of DSBs (*2*, *3*), play distinct roles in DSB repair. The sequence of the hMre11-hRad50 complex is similar to the bacterial exonuclease SbcCD sequence (*18*), which suggests that this complex functions as an exonuclease that may be involved in the processing of DNA ends before strand exchange and religation (*19*–*21*). Because hRad51, a human RecA homolog, mediates DNA strand exchange (*22*), its action is likely to be required later than that of the hMre11-hRad50 protein complex in DSB repair. Null *Scmre11* and *Scrad51* mutations in *Saccharomyces cerevisiae* indicate that the yeast Mre11-Rad50-Xrs2 complex, but not ScRad51, plays an important role in nonhomologous end joining in this organism (*19*, *21*). Finally, both biochemical and cytologic experiments indicate that hRad51 is not physically associated with the hMre11-hRad50 complex (*2*).

To determine whether partial volume irradiation could distinguish the actions of hRad51 and hMre11 in intact nuclei, we doubly stained cells for DSBs (FITC–anti-BrdU) and hMre11 (antihMre11) (*23*). Analysis of stripe-irradiated doubly stained 37Lu cells revealed that, as early as 30 min after irradiation, the BrdU-labeled DSBs and hMre11 protein colocalized (Fig. 3). The abundance and composition of the hMre11-hRad50 complex are identical in irradiated and unirradiated cells (*2*, *24*). Hence, the association of these proteins with damaged DNA was due to migration of existing hMre11-hRad50 complexes. Optical sectioning of hMre11 stripe-positive nuclei revealed that hMre11 protein was localized in stripes throughout the nuclear volume (*14*). The FITC signal (corresponding to DSBs) disappeared by 90 to 300 min after irradiation, whereas hMre11 staining became diffuse, as it is in unirradiated cells.

Vestigial hMre11 stripes persisted in about 5% of nuclei examined at 300 min (Fig. 4C). Previous studies of DSB repair in human cells have indicated that the bulk of ionizing radiation-induced DSBs are repaired within the first 60 min after irradiation and that a more slowly repaired population of DSBs persists for 24 to 48 hours (*16*, *25*). Our data suggest that the hMre11-hRad50 complex functions in the fast component of DSB repair. Because we previous-

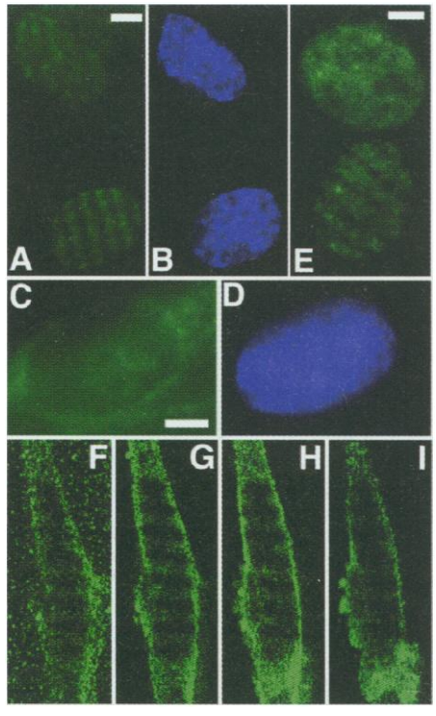

Fig. 2. Partial volume irradiation of 37Lu or 180BR human fibroblasts (*7*). Cells were labeled for DSBs with BrdU and FITC–anti-BrdU (A, C, and E), followed by DAPI (B and D) counterstaining (*10*). (**A** and **B**) 37Lu, 30 min after irradiation; bar, 5 μm; (**C** and **D**) 37Lu, 90 min after irradiation; bar, 5 μm; (**E**) 180BR, 5 hours after irradiation; bar, 5 μm; (**F** to **I**) optical sections of a partially irradiated 37Lu nucleus labeled for DSBs with BrdU (*10*). Representative images separated by 1.0 μm are shown (*13*), with increasing distance from the x-ray beam from (F) to (I). The high background observed in (F) is caused by autofluorescence from the Mylar plating surface.

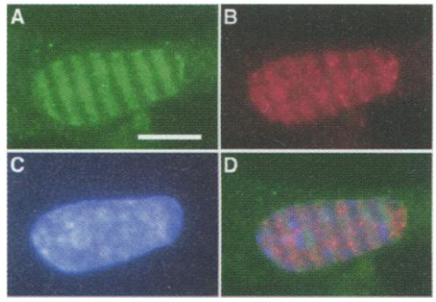

Fig. 3. Colocalization of BrdU incorporation and hMre11 stripes. Thirty minutes after irradiation, 37Lu fibroblasts were sequentially labeled (*23*) to detect BrdU (FITC–anti-BrdU) (**A**), hMre11 (**B**), and DNA (DAPI) (**C**). (**D**) Merged image of (A) to (C). Bar, 10 μm.

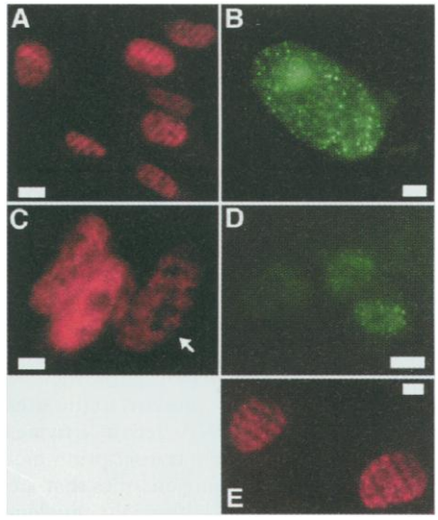

Fig. 4. Localization of hMre11 to stripes after partial volume irradiation. 37Lu (**A** to **D**) or 180BR (**E**) fibroblasts were fixed after partial volume irradiation and stained for hMre11 or hRad51 (*26*). (A) Anti-hMre11, 30 min after irradiation; (B) anti-hRad51, 30 min after irradiation; (C) anti-hMre11, 5 hours after irradiation; note that one nucleus (arrow) shows a weak stripe pattern; (D) anti-hRad51, 5 hours after irradiation; (E) anti-hMre11 in 180BR cells, 5 hours after irradiation. Bars in (A) and (D), 10 μm; bars in (B), (C), and (E), 5 μm.

ly showed that these proteins also function in the slower component of DSB repair (*2*), the residual hMre11 stripes may indicate that the number of slowly repaired DSBs falls below the limit of TdT detection, whereas immunofluorescent detection of hMre11 is sufficiently sensitive to identify these slower repair events.

To determine whether localization of hMre11 was attributable to the presence of DSBs, we examined whether persistent DSBs in irradiated DSB repair-deficient 180BR cells produced a longer lived signal for hMre11 localization. The hMre11 stripes were present in most irradiated 180BR cells as late as 300 min after irradiation (Fig. 4E), in contrast to the results with 37Lu cells. Thus, DSBs appear to constitute the signal for hMre11 localization.

We next investigated whether hMre11 and hRad51 colocalized at sites of DNA damage in stripe-irradiated 37Lu cells. Cells were fixed 30 and 300 min after irradiation and stained with antisera to hRad51 and hMre11 (*26*). As above, 30 min after irradiation, most (>90%) nuclei exhibited a striped pattern of hMre11 localization (Fig. 4A). About 10% of cells contained hRad51 foci 30 and 300 min after irradiation, but these foci did not form a striped pattern at either time point (Fig. 4, B and D). The failure of hMre11 and hRad51 to colocalize in irradiated stripes supports the assertion that these proteins mediate distinct functions in the DSB repair process, consistent with our previous cytologic analyses (*2*). The fraction of hRad51 focus-positive irradiated cells observed in these experiments was somewhat lower than in previous studies, presumably reflecting the low levels of hRad51 expression in the primary fibroblasts used for this study (*2*, *3*, *27*).

Our observations confirm that biologically relevant interactions of ultrasoft x-rays are confined to small intranuclear volumes (*8*, *28*) and provide physical evidence that the hMre11-hRad50 protein complex localizes to the sites of DNA damage. These findings indicate that the activation of DNA repair must include relocalization of repair proteins to the sites of DNA damage. DNA repair enzymes thus appear to resemble transcription factors and RNA processing enzymes that are proposed to migrate within the nucleus but are distinct from enzymes that mediate DNA replication from stationary replication factories (*1*, *29*).

Relocalization of the hMre11-hRad50 protein complex may indicate that signals originate from the site of DNA damage to recruit DNA repair enzymes. In this regard, the signal that activates DNA repair may be analogous to those that activate DNA damage-dependent cell cycle checkpoint functions (*30*). It has been suggested that the DNA-activated protein kinase trimeric complex (Ku70/Ku86/DNA-PKcs), which binds to DNA ends in vitro and induces protein phosphorylation activity, may signal the presence of DNA damage (*31*). Based on the failure to suppress DNA synthesis after ionizing radiation of cells established from ataxia telangiectasia patients, a similar function has been proposed for ATM (*32*). The use of mutants such as *dna-pk* and *ATM* in partial volume irradiation assays may help to define defects in signaling functions required for relocalization of DSB repair proteins.

REFERENCES AND NOTES

1. P. Hozak, A. B. Hassan, D. A. Jackson, P. R. Cook, *Cell* **73**, 361 (1993); J. Strouboulis and A. P. Wolffe, *J. Cell Sci.* **109**, 1991 (1996).
2. R. S. Maser, K. J. Monsen, B. E. Nelms, J. H. J. Petrini, *Mol. Cell. Biol.* **17**, 6087 (1997).
3. T. Haaf, E. I. Golub, G. Reddy, C. M. Radding, D. C. Ward, *Proc. Natl. Acad. Sci. U.S.A.* **92**, 2298 (1995).
4. R. Scully *et al.*, *Cell* **90**, 425 (1997).
5. M. S. Park *et al.*, *Proc. Natl. Acad. Sci. U.S.A.* **93**, 8368 (1996).
6. J. F. MacKay *et al.*, *Med. Phys.*, in press.
7. B. E. Nelms *et al.*, *Radiat. Res.*, in press.
8. R. P. Virsik-Peuckert, in *Radiation-Induced Chromosome Damage in Man*, I. Ishihara and M. S. Sasaki, Eds. (Liss, New York, 1983), vol. 4, pp. 51–69.
9. D. T. Goodhead, J. Thacker, R. Cox, *Int. J. Radiat. Biol.* **63**, 543 (1993).
10. Logarithmic-phase human fibroblasts plated on 8-μm Mylar were irradiated (*7*) with a mean nuclear dose (*D*) of 100 Gray. The dose was calculated by using the known entrance dose (D_s), the attenuation coefficient (μ) of 1.34 keV x-rays in cells (0.19 mm^{-1}), and the estimated cell thickness [T_n = nuclear thickness (5 μm), T_c = cytoplasmic thickness (0.5 μm) (*13*)] in the equation $D = (D_s/\mu T_n)(e^{-\mu Tc} - e^{-\mu(Tc+Tn)})$. Cells were fixed and permeabilized 30 min, 90 min, or 5 hours after irradiation as described in (*12*). (Technical limitations precluded analysis of cells earlier than 30 min after irradiation.) Cells were briefly washed in double-distilled H_2O and incubated for 60 min at 37°C in labeling mixture [100 mM sodium cacodylate (pH 7.6), 1 mM $CoCl_2$, 0.2 mM dithiothreitol, 0.005% Triton X-100, 45 nmol of BrdU per milliliter, 250 units of TdT (Promega, Madison, WI)]. Labeling reactions were stopped by rinsing with tris-buffered saline (TBS) [100 mM tris-HCl (pH 7.5) containing 150 mM NaCl] and cells were incubated for 20 min at 37°C in a blocking solution consisting of 2% bovine serum albumin and 0.3% Triton X-100 in TBS, followed by a 30-min incubation at 37°C with 6.25 mg of FITC–anti-BrdU (Becton Dickinson) per milliliter in blocking solution. Cells were washed for 10 min in three changes of fresh TBS, counterstained with 4′,6-diamidino-2-phenylindole (DAPI) (0.1 μg/ml), and mounted in antifade solution [2.3% diazabicyclo{2.2.2}octane, 90% (v/v) glycerol, 10 mM tris-HCl (pH 7.5)].
11. X. Li and Z. Darzynkiewicz, *Cell Prolif.* **28**, 571 (1995).
12. R. Kodym and E. Hurth, *Int. J. Radiat. Biol.* **68**, 133 (1995).
13. Optical sectioning was carried out with a Bio-Rad MRC600 confocal microscope system (using the FITC filter set; ×60, 1.4 numerical aperture objective). Z-series (in the plane perpendicular to the x-ray beam direction) were collected with a step size of 0.5 μm starting from the plating surface (beam proximal). The average cell thickness was 5 to 5.5 μm. The resulting stacks were viewed and contrast enhanced with NIH Image 1.61 (ftp://codon.nih.gov/pub/nih-image/). Individual sections were then extracted into Photoshop 4.0 (Adobe).
14. B. Nelms, R. Maser, J. Petrini, data not shown.
15. Neutral comet assays (*2*) were carried out on human 37Lu fibroblasts after partial volume irradiation. The amount of DSBs remaining in cells observed 5 hours after irradiation (mean tail moment 11.5) was comparable to that in unirradiated controls (mean tail moment 12.9) and was less than the amount of DSBs observed 30 min after irradiation (mean tail moment 50.8).
16. S. W. Botchway, D. L. Stevens, M. A. Hill, T. J. Jenner, P. O'Neill, *Radiat. Res.* **148**, 317 (1997).
17. C. Badie *et al.*, *ibid.* **144**, 26 (1995); C. Badie *et al.*, *Cancer Res.* **55**, 1232 (1995).
18. D. R. Leach, *Bioessays* **16**, 893 (1994); G. J. Sharples and D. R. Leach, *Mol. Microbiol.* **17**, 1215 (1995); J. C. Connelly and D. R. Leach, *Genes Cells* **1**, 285 (1996).
19. R. Kanaar and J. H. J. Hoeijmakers, *Genes Function* **1**, 165 (1997).
20. J. W. Szostak, T. L. Orr-Weaver, R. J. Rothstein, F. W. Stahl, *Cell* **33**, 25 (1983); N. Sugawara and J. E. Haber, *Mol. Cell. Biol.* **12**, 563 (1992); E. L. Ivanov, N. Sugawara, C. I. White, J. E. Haber, *ibid.* **14**, 3414 (1994).
21. J. H. J. Petrini, D. A. Bressan, M. S. Yao, *Semin. Immunol.* **9**, 181 (1997).
22. P. Sung and D. L. Robberson, *Cell* **82**, 453 (1995); P. Baumann, F. Benson, S. C. West, *ibid.* **87**, 757 (1996); R. C. Gupta, L. R. Bazemore, E. I. Golub, C. M. Radding, *Proc. Natl. Acad. Sci. U.S.A.* **94**, 463 (1997).
23. After treatment with FITC–anti-BrdU (*10*), cells were washed in phosphate-buffered saline and then blocked and stained with antisera as in (*2*) except that Lissamine Rhodamine–conjugated antibody to rabbit immunoglobulin (Jackson ImmunoResearch, West Grove, PA) was substituted for FITC-conjugated secondary antisera.
24. G. M. Dolganov *et al.*, *Mol. Cell. Biol.* **16**, 4832 (1996).
25. M. N. Cornforth and J. S. Bedford, *Science* **222**, 1141 (1983); B. Nevaldine *et al.*, *Radiat. Res.* **133**, 370 (1993); M. Lobrich, B. Rydberg, P. K. Cooper, *Proc. Natl. Acad. Sci. U.S.A.* **92**, 12050 (1995).
26. 37Lu or 180BR fibroblasts were plated and irradiated (*10*), fixed in 4% paraformaldehyde in 200 mM sucrose containing PBS (pH 7.4) for 5 min, and then permeabilized for 5 min (*4*). Cells were incubated in blocking solution and then treated with anti-hMre11 or anti-hRad51 or double-labeled with anti-hRad51 plus Texas Red–conjugated anti-hMre11 (*2*). Images were captured under epifluorescence with a cooled charge-coupled device camera and images were processed using Photoshop 4.0 (Adobe).
27. A. Yamamoto *et al.*, *Mol. Gen. Genet.* **251**, 1 (1996); J. Flygare, F. Benson, D. Hellgren, *Biochim. Biophys. Acta* **1312**, 231 (1996).
28. R. Cox, J. Thacker, D. T. Goodhead, *Int. J. Radiat. Biol.* **31**, 561 (1977); D. T. Goodhead, J. Thacker, R. Cox, *ibid.* **36**, 101 (1979).
29. R. H. Singer and M. R. Green, *Cell* **91**, 291 (1997).
30. W. G. Nelson and M. B. Kastan, *Mol. Cell. Biol.* **14**, 1815 (1994); L. C. Huang, K. C. Clarkin, G. M. Wahl, *Proc. Natl. Acad. Sci. U.S.A.* **93**, 4827 (1996).
31. M. F. Hoekstra, *Curr. Opin. Genet. Dev.* **7**, 170 (1997); S. P. Jackson, *Cancer Surv.* **28**, 261 (1996); P. Jeggo, G. E. Taccioli, S. P. Jackson, *Bioessays* **17**, 949 (1995); D. T. Weaver, *Trends Genet.* **11**, 388 (1995).
32. Y. Shiloh, *Annu. Rev. Genet.* **31**, 635 (1997).

33. We thank our colleagues for materials and advice. Supported by the American Cancer Society (grant NP-918) and the Howard Hughes Medical Institute (J.H.J.P.), NIH grants 5T32GM07133 (R.S.M.) and 5T32GM08349 (B.E.N.), and the Air Force Office of Scientific Research and the National Science Foundation (grant DMR-9212658) (J.F.M. and M.G.L.). This work was conducted at the Synchrotron Radiation Center, University of Wisconsin. Paper number 3502 from the University of Wisconsin–Madison Laboratory of Genetics. This paper is dedicated to the memory of our friend and colleague, Tony Bladl.

4 November 1997; accepted 10 March 1998